Bulgarian Chemical Communications, Volume 49, Special Edition K2, (pp. 200 – 206) 2017

Ecological response to land use change: a case study from the Chaohu lake basin, China

B. Wang[1,2], L. Chen[1*], L. Li[1,3], H. Xie[4], Y. Zhang[1]

[1] *School of Environment Science and Spatial Informatics, China University of Mining and Technology, Xuzhou 221116, China*

[2] *Anhui Province Institute of Land Surveying and Planning, Hefei 230631, China;*

[3] *Department of Geography, Earth System Science, Vrije Universiteit Brussel, Brussels 1050, Belgium*

[4] *School of Environment and Energy Engineering, Anhui Jianzhu University, Hefei, 230601, China*

Received August 15, 2017, Revised November 15, 2017

Land use change (LUC) has been considered as a major cause of global environmental change. Characterizing LUC and its impact on the eco-environment can contribute to the sustainability of regional development. In order to accurately assess the ecological response to LUC, this study proposed a land use change and ecological response (LUCER) framework by means of remote sensing, incorporating the land use transition matrix, remote sensing ecological index (RSEI), and spatial regression methods. The LUCER framework was tested on the Chaohu lake basin. Results showed that the LUC intensity of the study area increased significantly, but RSEI decreased by a large margin, and the change trend showed a U shape. Moreover, LUC was the Granger cause of RSEI and their correlation remained negative. The LUCER framework performed well in measuring the LUC and RSEI changes. Our research suggests that the LUCER framework could effectively explain the dynamic process and functioning mechanisms of LUC and RSEI changes and quantitatively evaluate the LUC ecological response. From an ecological environment protection perspective, the results of this study can provide an insight into land use decision-making for policy makers.

Key words: Land use change; Remote sensing ecological index; Ecological response

INTRODUCTION

As a physical basis of various ecosystems, land serves as the most direct link between humans and nature. Land use change (LUC) has been closely connected with global environmental change and development sustainability [1]. By changing the structure and functions of an ecosystem, LUC can further impact its services [2]. The ecological impact of LUC, which is important to human wellbeing, has escalated in recent years. In general, LUC can be divided into two types, namely, implicit change and explicit change. The former refers to structural change, such as the change in the quantitative scale and spatial structure, whereas the latter, which is dependent on the former, reflects the change in quality, function, input, output, and so on. Economic growth is one of the main drivers of LUC and the overall impact of LUC on the eco-environment is negative. From 1978 to 2016, the urbanization rate in China rose from 17.9% to 57.4%, with an annual growth rate of 1.04%. However, China's ecologically vulnerable areas accounted for more than 60% of its total territory in 2014. As such, the Chinese government is committed to the construction of ecological civilization. In response to the central government's call, the research scope of LUC should be further expanded, for example, to cover the changes in land ecosystems.

To date, LUC and ecological changes have been long investigated but researchers have mainly focused on the characteristics and effects of LUC and ecological index changes. LUC or ecological change data are often extracted from remote sensing or simulated by CLUE-S and CA-Markov models [3,4]. From the perspective of biological habitats and resource distribution, Fu *et al*. [5] concluded that land use pattern can impact ecosystem services. Meanwhile, LUC is also considered responsible for soil erosion [6,7], frequent flooding [8], and urban heat island [9]. In addition, ecological indices, which can directly reflect eco-environmental quality, have been increasingly used to study ecological quality change. Xu [10] developed the remote sensing ecological index (RSEI) for evaluating the ecological quality of Chinese cities and suggested its wide application. Most of the abovementioned research described the correlation between LUC and ecological change while they did not reveal the impact of LUC on ecosystems in a systematical manner. Additionally, these studies mainly used remote sensing image data of two different years, which is insufficient to provide an accurate assessment and an overview understanding of the ecological quality change.

This study therefore presents a framework of land use change and ecological response (LUCER) to evaluate the impact of the LUC on regional

To whom all correspondence should be sent:
E-mail: chenlq@cumt.edu.cn

ecological changes. Remote sensing image data acquired in four different years (2000, 2005, 2010 and 2015) were used for deriving land use cover maps and RSEI. LUC and RSEI change were then characterized through the land use transition matrix and statistical measures and then their relationships were modeled by linear regression.

EXPERIMENTAL

Materials

Drainage basins are usually densely populated areas with highly intensive land use and the Chaohu Lake Basin is one of the examples. The Chaohu Lake is located in the center of the eastern Chinese province of Anhui (Fig. 1) and profiled as one of the five fresh water lakes in China. The Chaohu Lake Basin consists of 14 districts/counties among which nine belong to the provincial capital city of Hefei – one of the centers in the Yangtze River delta mega-city region. In 2016, the Chaohu Lake Basin registered 11.37 million permanent residents, with an urbanization rate of 65.97%. The basin covers a geographical area of 1.97×10^4 km^2, 3.8% of which is the water surface of the Chaohu Lake. Lying on the Yangtze River-Huai River hilly belt, the basin is characterized by elevations in the west and lowland in the east (Fig. 1c). The subtropical moist monsoon climate has resulted in the formation of 33 rivers of different lengths. Due to increasing human activity, water blooms have rapidly spread in these rivers. It was estimated in 2016 that water blooms affected 31.99% (237.6 km^2) of the total lake surface.

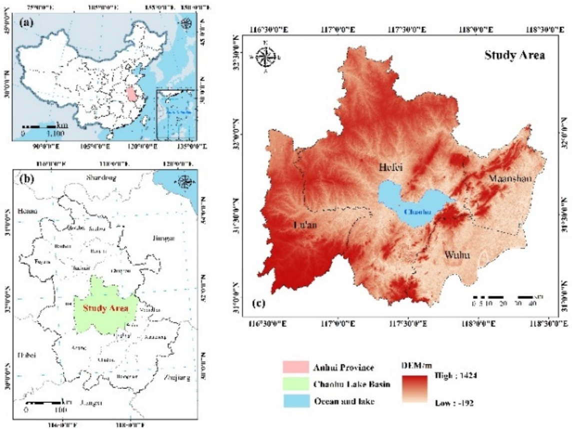

Fig. 1. Location of the study area: (a) Anhui province in China; (b) Chaohu lake basin in Anhui province; (c) elevation map of the study area with the Chaohu lake highlighted in blue. The study area covers part of four Anhui cities, namely Hefei, Maanshan, Wuhu, and Lu'an.

Data used in this study include remote sensing images and DEM data. They were used to interpret land use cover maps and derive RSEI. Table 1 shows the details of the four remote sensing images (i.e. 2000, 2005, 2010 and 2015).

Table 1. Remote sensing image data of the study area used for deriving RSEI

Date	Scene	Acquisition date	Path/Row
2000	Landsat 5 TM	10 October 2000	120/38; 121/38
2005	Landsat 5 TM	24 October 2005	120/38; 121/38
2010	HJ-1B-CCD	31 October 2010	452/76; 452/80; 457/76; 457/80
2015	HJ-1B-1RS	18 October 2015	455/70
	HJ-1B-CCD		454/76
	HJ-1B-1RS		456/77

The Landsat 5 TM data were downloaded from the Geospatial data cloud (http://www.gscloud.cn/) and the HJ-1B data were from the China Center for resources satellite data and application (http://www.cresda.com/). Landsat 5 TM and HJ-1B sensors have identical spatial resolutions (i.e. 30 m) with basically consistent spectral ranges, which allows their data to substitute each other [11]. All these cloud-free images were acquired in October, guaranteeing that vegetation was at nearly the same growth stage. Pre-processing of the Landsat 5 TM and HJ-1B image data such as clipping, radiation correction, and geometric correction was performed in ENVI 5.1. The DEM covering of the study area was produced by mosaicking 30-m-resolution DEM datasets from the ASTER GDEM V2 (N30E116; N31E116; N31E117; N31E118; N32E116; N32E117; N32E118) in ArcGIS 10.2. Based on the *Codes for the Current Land Use Classification in China (GB/T21010-2007)*, the remote sensing data were classified using a SVM (support vector machine) and land use was divided into six Level-1 types: arable land, forest land, grass land, waters, land for urban and rural construction, and other land. Among them, arable land was further divided into two Level-2 types (paddy field and unirrigated field), and land for urban and rural construction into three Level-2 types (urban residential land, rural residential land, and industry-traffic land). The accuracy assessment results showed that the Kappa indexes for each time period for arable land, forest land and waters, etc. were larger than 0.8, and the Kappa index for grass land was 0.75. The accuracy of classification conformed to the requirement of the study.

Analytical methods

Land use transition matrix

The land use transition matrix was used to represent the transition between different land use types (Table 2). The row represents the land use type A_i at time T_1, while the column represents the land use type A_j at time T_2. The matrix element C_{ii} represents the constant area of land use type i from T_1 to T_2 while the matrix element C_{ij} represents the area of land use type i, which is transitioned into land use type j from T_1 to T_2, and P_{ij} denotes the percentage of the transition.

Table 2. Land use transition matrix

T_1	T_2					
	A_1	A_2	···	A_j	···	A_n
A_1	C_{11}	C_{12}	···	C_{1j}	···	C_{1n}
	P_{11}	P_{12}	···	P_{1j}	···	P_{1n}
A_2	C_{21}	C_{22}	···	C_{2j}	···	C_{2n}
	P_{21}	P_{22}	···	P_{2j}	···	P_{2n}
⋮	⋮	⋮	⋮	⋮	⋮	⋮
A_i	C_{i1}	C_{i2}	···	C_{ij}	···	C_{in}
	P_{i1}	P_{i2}	···	P_{ij}	···	P_{in}
⋮	⋮	⋮	⋮	⋮	⋮	⋮
A_n	C_{n1}	C_{n2}	···	C_{nj}	···	C_{nn}
	P_{n1}	P_{n2}	···	P_{nj}	···	P_{nn}

In order to investigate how much a land use type (i) was transitioned into another land use type (j), we proposed a measure termed transition rate (TR_j):

$$TR_j = \frac{GA_j}{LA_i} \tag{1}$$

where LA_i is the total lost area of land use type i over the period, GA_j is the area of land use type j that is gained through transition from land use type i.

Remote sensing ecological index

The RSEI is a function of greenness, wetness, heat and dryness that human beings can directly feel in the environment. The four components can be represented by different remote sensing based measures, namely the normalized difference vegetation index (NDVI), wet index (WI), land surface temperature (LST), and normalized different built-up soil index (NDBSI). Therefore, the function can be expressed by:

$$RSEI = f(NDVI, WI, LST, NDBSI) \tag{2}$$

The four components in the function are given as follows:

(1) The NDVI is a vegetation index that provides vegetation biomass information can be calculated by [12]:

$$NDVI = \frac{\rho_{NIR} - \rho_{red}}{\rho_{NIR} + \rho_{red}} \tag{3}$$

where ρ_{NIR} and ρ_{red} are reflectance in the near infrared and red bands of Landsat 5 TM (or HJ-1B) data. Variables such as ρ_{green}, ρ_{blue}, ρ_{LWIR} and ρ_{SWIR} in the following equations have similar meaning.

(2) The WI is a humidity component obtained through a tasseled-cap transform. Calculation of WI varies with sensor type.

For Landsat 5 TM data, WI can be obtained by [13]:

$$WI = 0.03\rho_{blue} + 0.20\rho_{green} + 0.31\rho_{red} + 0.16\rho_{NIR} - 0.68\rho_{SWIR1} - 0.61\rho_{SWIR2} \tag{4}$$

For HJ-1B data, it can be obtained by [14]:

$$WI = -0.14\rho_{blue} + 0.004\rho_{green} + 0.73\rho_{red} - 0.67\rho_{NIR} \tag{5}$$

(3) LST can be derived from remote sensing imagery through the method presented in the study of Nichol [15]. However, it was substituted by brightness temperature (BT) for simplicity in this study because BT approximates it [16] and accurate calculation of land surface temperature is not the main target. BT was computed by [17]:

$$BT = \frac{K_2}{\ln\left(1 + {K_1}/{\rho_{LWIR}}\right)} \tag{6}$$

where K_1 = 607.76 $W/(m^2 \cdot sr \cdot \mu m)$ and K_2 = 1260.56 K for Landsat 5 TM data [17], and K_1 = 579.20 $W/(m^2 \cdot sr \cdot \mu m)$ and K_2 = 1245.58 K for HJ-1B data [18].

(4) The normalized different building-soil index (NDBSI) is the average of the built-up index (BI) and the soil index (SI) [19]:

$$NDBSI = \frac{SI + IBI}{2} \tag{7}$$

where SI and BI can be computed by [19], respectively:

$$SI = \frac{(\rho_{SWIR1} + \rho_{red}) - (\rho_{blue} + \rho_{NIR})}{(\rho_{SWIR1} + \rho_{red}) + (\rho_{blue} + \rho_{NIR})} \tag{8}$$

$$IBI = \frac{2\rho_{SWIR1}/(\rho_{SWIR1} + \rho_{NIR}) - \left[\rho_{NIR}/(\rho_{NIR} + \rho_{red}) + \rho_{green}/(\rho_{green} + \rho_{SWIR1})\right]}{2\rho_{SWIR1}/(\rho_{SWIR1} + \rho_{NIR}) + \left[\rho_{NIR}/(\rho_{NIR} + \rho_{red}) + \rho_{green}/(\rho_{green} + \rho_{SWIR1})\right]} \tag{9}$$

Because our focus was on the area around the Chaohu Lake and water affects the calculation of the four components, surface water was masked out [10]. In addition, the four components varied in units and range of values, they were normalized to the 0-1 range. Here we applied Eq. (10) to the NDVI and WI and applied Eq. (11) to LST and NDBSI:

$$Y_i = \frac{X_i - Min_i}{Max_i - Min_i} \tag{10}$$

$$Y_i = \frac{Max_i - X_i}{Max_i - Min_i} \tag{11}$$

where X_i and Y_i are the original and normalized values of the four components, respectively; Max_i and Min_i are the maximum and minimum values of the four components, respectively. It is noted that greenness and wetness have positive effects on the environment while heat and dryness have negative effects on the environment.

To exclude the impact of artificially introduced weights on RSEI estimation, Xu [10] reported that their weights can be obtained through their principal component analysis (PCA). Through PCA, most of the normalized measures were explained by the first principal component (PC1):

$$PC1 = a \times Normalized\ NDVI + b \times Normalized\ WI + c \times Normalized\ LST + d \times Normalized\ NDBSI \quad (12)$$

where a, b, c, and d are the coefficients of the normalized measures, which could be used as their corresponding weights for calculating the RSEI. In this case, the PC1 was actually the RSEI.

However, such coefficients vary from imagery to imagery, which suggests that the RSEI of the study area in different years would be obtained from different functions. This does not allow a direct comparison of the RSEI of different years. To solve this problem, we proposed a new simple method to determine the weights by averaging their values of different years, e.g. $a = (a_{2000} + a_{2005} + a_{2010} + a_{2015})/4$. Finally, the RSEI was also normalized to the 0-1 range for zoning and comparison. After normalization, a higher RSEI value indicates a better ecological quality and *vice versa*.

Spatial multiple regression based on geographical grid

In order to identify LUC hot spots, and analyze the percentage of LUC and the corresponding RSEI change values, we built a geographical grid for the study area. For a more effective ecological quality evaluation, the size of the grid unit is recommended to be 2 to 3 times larger than the average patch area of the study area [20]. As the average patch area of the study area was 4.23 km^2, the size of the grid unit was set at 3 km × 3 km – the study area was covered by a total of 2,400 grid units. A simple regression model of RSEI was constructed with the percentage of LUC area in a grid unit. These variables were computed within the grid unit if it was completely within the study area.

LUCER framework

By integrating all the above-mentioned measures and methods, we proposed a LUCER framework to evaluate the impact of the LUC on regional ecological changes. This framework consists of two parts: the first part was to derive LUC and RSEI from remote sensing image data, through land use classification and remote sensing based measures (NDVI, WI, LST, and NDBSI), respectively. The second part was to identify hotspots of LUC and RSEI changes. The Granger analysis and the spatial regression analysis based on the geographical grid were combined to examine the interaction between LUC and RSEI change. Through this model, the mechanism of ecological response to LUC was revealed.

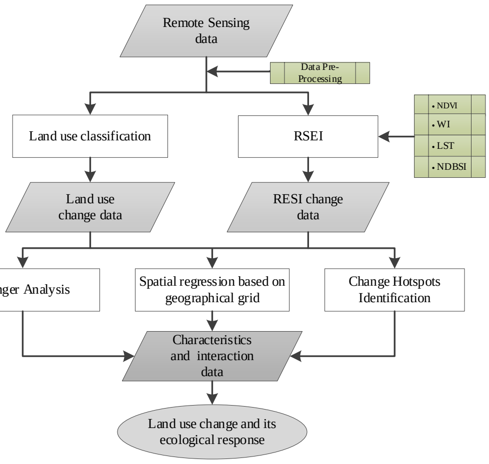

Fig. 2. Structure of LUCER framework presented in this study

RESULTS AND DISCUSSION

Characterizing land use change

From land use cover maps for 2000, 2005, 2010 and 2015 (Fig. 3) it was clear that arable land was the major land use type, accounting for 68.19%, 67.64%, 65.87%, and 63.66% of the total area for the four years, respectively.

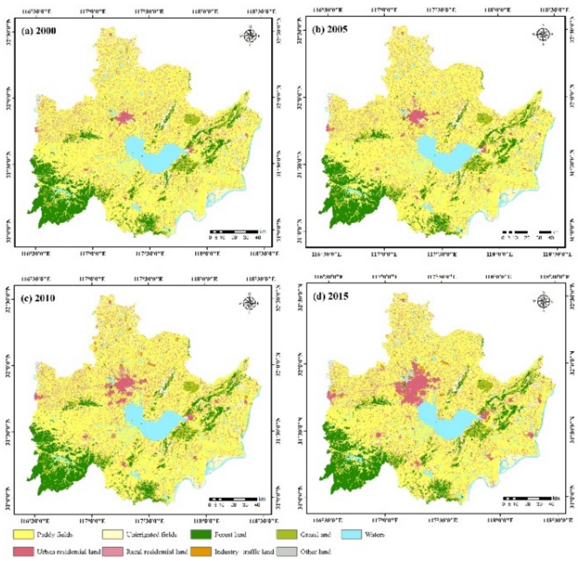

Fig. 3. Land use cover maps

However, the arable land continuously shrank while land for urban and rural construction increased steadily, with a growth rate of 41.30%. The increase in the area of land use for urban and rural construction was 91.66% of the decrease in the area of arable land. This suggests that the expansion of land for urban and rural construction was a major cause of arable land decrease for the period from 2000 and 2015.

Table 3 shows that paddy field, unirrigated field, rural residential land and industry-traffic land were the main land use types that experienced significant changes from 2000 to 2015, all their change rates being higher than 5%. It illustrates that:

(1) Urban residential land was a hotspot of land use transition. From 2005 to 2010, the transition of industry-traffic land was among the most dramatic ones – 4.99 km^2 (21.36%) were transitioned into urban residential land. This can be explained by the fact that industrial parks were mainly in suburbs, which were later incorporated into cities as a result of urban expansion.

(2) Most arable land was transitioned into land for urban and rural construction. From 2000 to 2005, the transition rate of unirrigated field transitioned into urban residential land was 85.50%. From 2010 to 2015, part of arable land was transitioned into waters. This change was made mainly in response to the policy for protection of the wetland and return farmlands to lakes.

(3) The land use transition of urban residential land was diversified. From 2000 to 2005 and from 2005 to 2010, the urban residential land was mainly reclaimed into paddy fields, and the transition rates were 77.65%, 50.14%, respectively. However, from 2010 to 2015, urban residential land started to transform into grass land and waters in accordance with eco-environment requirements.

Characterizing the RSEI change

Mean values of the normalized NDVI, WI, LST, NDBSI, and the RSEI of the study area were calculated for each year. The normalized NDVI was highest (0.57) in 2000 and fell in the following 10 years before rising to 0.53 in 2015. This suggested that the influence of afforestation projects in the study area from 2010 to 2015 was obvious. The normalized WI increased from 2005 to 2010 and decreased afterwards, with a highest value (0.63) in 2005. The normalized LST and NDBSI changed little over the 15 years. The RSEI changed in a similar way to the normalized NDVI.

The eigenvalue contributions of the first principal component (PC1) were all higher than 94%. This suggests that the first PC explains most of the variability of input normalized measures. However, the PC1 coefficients of the four normalized measures varied significantly. The differences between the maximum and minimum PC1 coefficients of normalized NDVI, WI, LST, and NDBSI were 28.95%, 18.60%, 43.14%, and 38.89%, respectively. Through averaging, the weight values of the

Table 3. Land use transition matrix of the study area from 2000 to 2015 (km^2, %)

	2000 - 2015								
	Paddy fields	Unirrigated field	Forest land	Grass land	Waters	Urban residential land	Rural residential land	Industry - traffic land	Other land
Paddy field	12013.14	16.43	12.68	13.95	95.04	385.08	305.45	104.86	4.37
	—	0.13	0.10	0.11	0.73	2.97	2.36	0.81	0.03
Unirrigated field	4.86	766.69	0.65	0.75	6.71	35.98	16.10	2.85	0.67
	0.58	—	0.08	0.09	0.80	4.31	1.93	0.34	0.08
Forest land	8.72	0.47	2136.46	3.85	2.50	0.65	6.12	4.54	0.39
	0.40	0.02	—	0.18	0.12	0.03	0.28	0.21	0.02
Grass land	2.64	0.20	3.37	747.73	1.25	0.02	7.86	7.68	0.01
	0.34	0.03	0.44	—	0.16	0	1.02	1.00	0
Waters	16.46	2.48	0.17	0.60	1436.14	3.65	1.37	1.03	0.00
	1.13	0.17	0.01	0.04	—	0.25	0.09	0.07	0
Urban residential land	0.26	0.06	0.00	0.00	0.49	193.05	0.03	0.01	0.00
	0.13	0.03	0	0	0.25	—	0.02	0.01	0
Rural residential land	31.15	5.94	0.28	1.21	3.13	52.99	1710.64	10.16	0.45
	1.72	0.33	0.02	0.07	0.17	2.92	—	0.56	0.02
Industry-traffic land	0.42	0.04	0.02	0.01	0.00	4.99	0.07	17.81	0.00
	1.80	0.17	0.09	0.04	0	21.36	0.30	—	0
Other land	0.01	0.00	0.01	0.01	0.00	0.00	0.00	0.00	0.93
	1.04	0	1.04	1.04	0	0	0	0	—

different measures were obtained, which were 0.22, 0.24, 0.32, and 0.22, respectively. Using the natural breaks method, the RSEI images were classified into five levels, namely, worst (0-0.2), worse (0.2-0.4), medium (0.4-0.6), better (0.6-0.8), and best (0.8-1) (Fig. 4.).

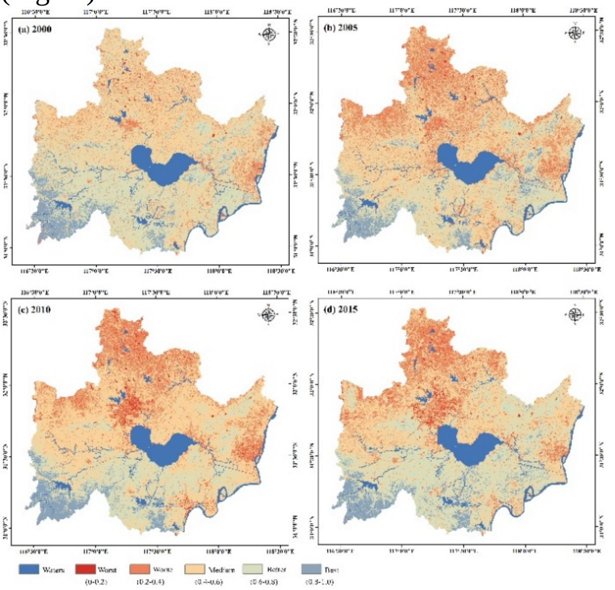

Fig. 4. The RSEI maps of the study area in 2000, 2005, 2010, and 2015

The percentages of the medium level and above were 90.11%, 78.96%, 80.09%, and 82.49% in 2000, 2005, 2010 and 2015, respectively. As such, the RSEI showed a U-shaped trend with a rapid drop in the 2000-2005 period and a slow increase in the 2005-2015 period. This suggested that the ecological quality was seriously worsened before gradual improvement. It was also noted that the medium level remained the largest one over the 15 years, accounting for at least 40%.

A comparative difference analysis was conducted on the RSEI classification maps. In the analysis, numbers from 1 to 5 were assigned to the levels from the worst to the best for differencing. Differencing result ranging from -1 to -4 was considered as worsening (indicated in red in Fig. 5.), and differencing result ranging from 1 to 4 was considered as improvement (green), while the 0 value was considered as consistency (white).

From 2000 to 2015, the worsening area was 5,854 km^2 (29.72% of the total RSEI area) while the improvement area was 3,900.10 km^2 (19.80%). From 2005 to 2010, the worsening trend was alleviated as the worsening area was only 1.18 times larger than the improvement area. From 2010 to 2015, the worsening area was however reduced to only half of the improvement area – the ecological quality was significantly improved during this period. The contrasting change over the 15 years was consistent with our knowledge of the study area: the eco-environment of the Chaohu lake basin was first partly damaged and then recovered.

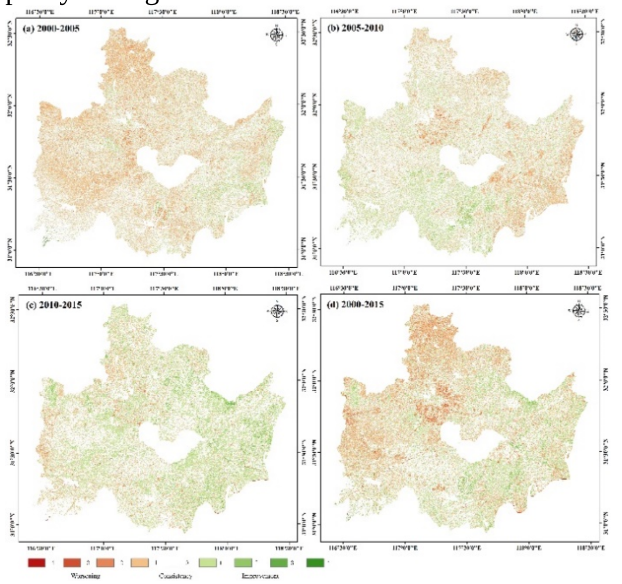

Fig. 5. The RSEI differencing

Modeling the interaction between land use change and RSEI change

The LUC types with a transition rate higher than 5% were treated as LUC hotspots, including paddy into urban land (32.25%), paddy into rural residential land (25.58%), and paddy into industry-traffic land (8.78%). Thus, the overall land use transition rate was 66.61%. The change process exerted a similar influence on the ecological quality. For example, the underlying surface conditions changed and the surface runoff increased, which led to changes in ecological system structure and services, decline of biological diversity maintenance, and weakening of adjustment capability. Therefore, the above change can be explained by the transition of paddy into land for urban and rural construction. The scatter plot of the percentage of the land use transition in the grid against the RSEI change value on the grid reveals their negative correlation ($R^2 = 0.82$) (Fig. 6.).

The Granger test showed that, at the significance level of 5%, X was the Granger cause of Y ($F = 70.52$, $P < 0.05$). This means that the transition of paddy into land for urban and rural construction was a major cause of the declining RSEI. The regression model meant that the increase in the transition of paddy into land for urban and rural construction in the geographical grid by 1% (0.09 km^2) would lead to a decrease in the overall RSEI by 12.91 in the geographical grid. The ecological quality decline was obvious.

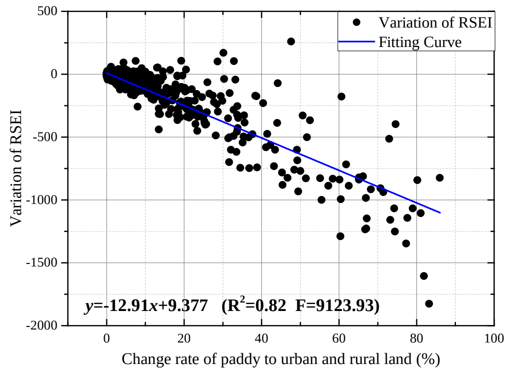

Fig. 6. Scatter plot of variation of RSEI against change rate of paddy to urban and rural residential land ($R^2 = 0.82$).

CONCLUSIONS

To achieve an accurate assessment of the ecological response to LUC, we used Landsat 5 TM and HJ-1B remote sensing imagery to build the land use change and ecological response (LUCER) framework and tested it on the Chaohu Lake Basin. Through the results, we have concluded that:

(1) The land use change analysis shows an increasingly dramatic LUC in the study area from 2000 to 2015. The change hot spots were reflected as quality arable land transitioned into land for urban and rural construction. During the 15 years, the RSEI dropped significantly, and the change trend presented a U shape. This was consistent with the true facts.

(2) The Granger test and the regression model based quantitative analysis indicated that LUC was the Granger cause of the RSEI change. LUC and RSEI change were negatively correlated. The government should monitor the LUC to control the land development and utilization of the area nearby.

(3) The LUCER framework can effectively explain the dynamic change process of land use and RSEI, reflect the interaction between the LUC and the RSEI change, predict the trend of LUC and RSEI change, and provide technical support for land management decision-making.

The LUCER framework can facilitate the analysis of the regional land use ecological response mechanism and characteristics, and improve the comprehensive effectiveness of regional land use management and ecosystem protection both in theory and in practice. However, LUC is not the only factor that triggers ecological change. Land utilization also has a potential influence on ecological change. It is recommended that further research should focus on the combined influence of LUC and land utilization on ecological quality to reveal the LUCER mechanism in depth.

Acknowledgements: *This study was financially supported by Public Science and Technology Project of Land and Resources of China (201411006-03).*

REFERENCES

1. E. Lambin, A. Veldkamp, *Glob. Chang. Newsl.*, **2**, 147 (2005).
2. T. Hasegawa, S. Fujimori, A. Ito, K. Takahashi, T. Masui, *Sci. Total Environ.*, **580**, 787 (2017).
3. T. Xia, W. Wu, Q. Zhou, P. H. Verburg, Q. Yu, P. Yang, L. Ye, *J. Geogr. Sci.*, **26**, 173 (2016).
4. B. Abuelaish, M.T.C. Olmedo, *Arab J. Geosci.*, **9**, 274 (2016).
5. B. Fu, S. Wang, C. Su, M. Forsius, *Curr. Opin. Environ. Sustain.*, **5**, 10 (2013).
6. V. Simonneaux, A. Cheggour, C. Deschamps, F. Mouillot, O. Cerdan, Y.L. Bissonnais, *J. Arid. Environ.*, **122**, 73 (2015).
7. M. Zare, T. Panagopoulos, L. Loures, *Land Use Policy*, **67**, 568 (2017).
8. J. Liu, Z. Shi, *Land Use Policy*, **65**, 206 (2017).
9. X. Du, Z. Huang, *Ecol. Indic.*, **81**, 243 (2017).
10. H. Xu, *China Environ. Sci.*, **33**, 891 (2013).
11. J. Luo, J. Zhang, W. Huang, G. Yang, X. Gu, H. Yang, *Spectroscopy Spectr. Anal.*, **30**, 3287 (2010).
12. J.W. Rouse, R.H. Hass, J.A. Schell, D.W. Deering, *Third Earth Resour. Technol. Satell. Symp.*, **1**, 310 (1974).
13. E. P. Crist, *Remote Sens. Environ.*, **17**, 303 (1985).
14. P. Cui, D. Li, C. Ma, *J. Taiyuan Univ. Technol.*, **47**, 316 (2016).
15. J. Nichol, *Photogramm. Eng. Remote Sens.*, **71**, 613 (2005).
16. Y. Zhang, L. Chen, Y. Wang, L. Chen, F. Yao, P. Wu, B. Wang, Y. Li, T. Zhou, T. Zhang, *Remote Sens.*, **7**, 10740 (2015).
17. Z. Qin, A. Karnieli, P. Berliner, *Int. J. Remote Sens.*, **22**, 3719 (2001).
18. S. Zhao, Q. Qin, F. Zhang, Q. Wang, Y. Yao, L. You, H. Jiang, R. Cui, Y. Yao, *Spectroscopy Spectr. Anal.*, **31**, 1553 (2011).
19. H. Xu, *Int. J. Remote Sens.*, **29**, 4269 (2008).
20. W. Zuo, G. Zhang, B. Wan, S. Li, Q. Wang, *Acta Geod. Cart. Sin.*, **32**, 269 (2003)